

BPC 00910

## AGGREGATION OF CHLOROPHYLLS IN MONOLAYERS

### VI. INFRARED STUDY OF THE C-H STRETCHING BANDS OF CHLOROPHYLL *a* AND OF CHLOROPHYLL *b* IN MONOLAYERS

Camille CHAPADOS

*Centre de recherche en photobiophysique, Université du Québec à Trois-Rivières, Trois-Rivières, Québec G9A 5H7, Canada*

Received 1st November 1983

Revised manuscript received 27th July 1984

Accepted 22nd October 1984

**Key words:** *Chlorophyll a; Chlorophyll b; Infrared spectroscopy; Monolayer; Photosynthesis*

The C-H vibrational stretch bands of chlorophyll (Chl) in monolayers, obtained by the Langmuir-Blodgett technique have been studied by infrared spectroscopy. Compared to a solution or to a multilayer which shows three to four bands, the spectra of Chl *a* or Chl *b* molecules in monolayers have revealed more than seven bands, which are assigned to the various CH groups in the molecule. In contrast to solutions or to multilayer samples which give featureless bands, each band of the monolayers is composed of many components which are modified when the system is perturbed either by drying or by hydration techniques. The separation between the components of the CH aliphatic bands is typical of crystalline field splitting and the modification of the intensities of these components is associated with the movement of the phytol chain of the chlorophyll molecules. The CH aromatic stretch bands have been observed; the displacement and variation of the intensities of these bands are associated with deformation of the porphyrin ring. The CH band of the formyl group on Chl *b* has also been observed. The displacement and variation of the intensity of this band are related to the association that this group makes with the surrounding molecules and with the displacement of the porphyrin ring.

## 1. Introduction

Carbonyl and magnesium groups have long been known to play an essential role in the aggregation state of the chlorophylls (Chl). Less attention has been paid to the C-H groups, but not because of a lack of them; indeed, there are 72. Perhaps they did not receive the attention they deserve because of too many different groups absorbing in a limited frequency range. Furthermore, much of the previous infrared spectroscopic work on Chl has been done in solution [1–5], in solids [6–10], or in multilayers [11–15], and these sampling techniques will necessarily integrate the absorption over many layers of Chl molecules in slightly different arrangements, which will broaden the bands; thus the individual components will become more difficult to observe.

With monolayers the situation is different. We have seen in refs. 12 and 15 that the aggregation state of Chl *a* is different in the multilayer, as compared to the monolayer. In the previous paper of this series [15], we have seen that the movement of the molecules in the monolayers is clearly distinguishable, since there is less integrating effect than in the other systems. In that paper, a close look at the carbonyl bands revealed many species, and in a dynamic situation, the absorbing components will be displaced from one frequency to another. In the same paper, a general survey of the C-H stretch region revealed some modifications in the absorption with modifications of the aggregation state.

In this paper, we will take a closer look at the C-H stretch region of the monolayer system of Chl *a* and of Chl *b*, using a greater resolution and an

abscissa scale expansion in order to resolve the individual components in different aggregation states. Through this process, our goal is to identify the different C-H vibrational stretching bands with the different C-H groups and the variation of these bands with the aggregation states.

## 2. Experimental

The materials, preparation of slides, deposition of monolayers, float trough, and the Langmuir film balance apparatus have been previously described in detail [17,18].

The extraction and purification of Chl *a* and Chl *b* from spinach leaves was performed by the standard method of Strain and Svec [19]. To determine the purity of the samples, we have used, as we did before [13], the following criteria: the surface pressure-area isotherm, the absorbance ratio of the blue to the red band, and thin-layer chromatography. Only those samples that had good criteria were used for the experiments.

Monolayers were obtained by depositing, at a surface pressure of  $20 \text{ mN m}^{-1}$ , one layer of Chl *a* or Chl *b* on each side of a multiple internal reflexion (MIR) germanium plate using the Langmuir film balance to monitor the deposition. Deposition took place on hydrophilic plates upon withdrawal only. Multilayers were obtained by depositing 40 layers of Chl *a* on a Ge hydrophobic MIR plate under the same conditions. The Chl monolayers were dried at  $65^\circ\text{C}$  under a vacuum of  $0.1 \text{ Pa}$ . The exposure to water vapor was done at  $25^\circ\text{C}$  in a closed container.

The infrared spectra were taken on a Perkin-Elmer model 180 spectrophotometer with a precision of  $\pm 1 \text{ cm}^{-1}$ . For the monolayers the resolution of the instrument was approx.  $2 \text{ cm}^{-1}$  and an ordinate scale expansion of 10 was used. For the multilayers, no ordinate scale expansion was used and the resolution was approx.  $3 \text{ cm}^{-1}$ . Several samples were studied. They all gave the same bands with the same satellite features. Only the intensities of the latter are slightly modified from one sample to another as the exact experimental conditions are difficult to duplicate.

### 2.1. Data manipulation

The experimental spectra were digitized using a Gradicon optical graph reader (Instronics Ltd., Stittsville, Ontario) and the data points stored on I.B.M. cards. The cards are fed into a Cyber 171 Control Data computer where the data are transformed to obtain the spectral values which are sent to a model 1051 Calcomp plotter (California Computing Products, Inc.) to obtain the spectra given in the figures.

## 3. Results and discussion

### 3.1. C-H vibrational bands of Chl in monomolecular arrays

In a multilayer of Chl *a* molecules, the C-H vibrational stretch bands are not very sensitive to small perturbations that the system suffers (figs. 3 and 8 of ref. 13). The position of these bands is given in table 1. A closer look at this table will show, however, that the maxima of the bands are slightly displaced from one system to another, and in system 2 (table 1) there are some small modifications within one system when the multilayer is dried. When the multilayer suffers more drastic modifications, such as the influence of water, the position of the bands (system 3 in table 1) varies somewhat more, but without drastic changes [15]. In a multilayer system, the absorption bands are integrated over all the layers, so that small displacements of the bands in one layer will not be clearly seen; only when most of the layers behave in the same way does the spectrum show some variations.

In a monolayer situation, there is no such integrating effect, and small perturbations in the environment of a functional group have a chance to be seen. In the carbonyl region, we have seen that these perturbations cause many modifications in the spectra [15]. On this basis we decided to have a closer look at the C-H stretching region of the monolayer systems using greater resolution, and with scale expansion of the ordinate and the abscissa.

The model of Chl *a* is given in fig. 1. This

figure is a drawing of the molecule using Dreiding stereomodels (Buchi). The distances between the atoms, and the ordering and numbering of the atoms are done according to the X-ray work of Kratky and Dunitz [16]. The orientation of the model has been made to simulate the Chl *a* mole-

cule at the air/water interface where the water of the trough is situated at the bottom of the figure. The orientation of the porphyrin ring is such as to make all the hydrogen bonds possible between the oxygen of the Chl molecule and the water molecules of the trough. Because of the hydrophobic

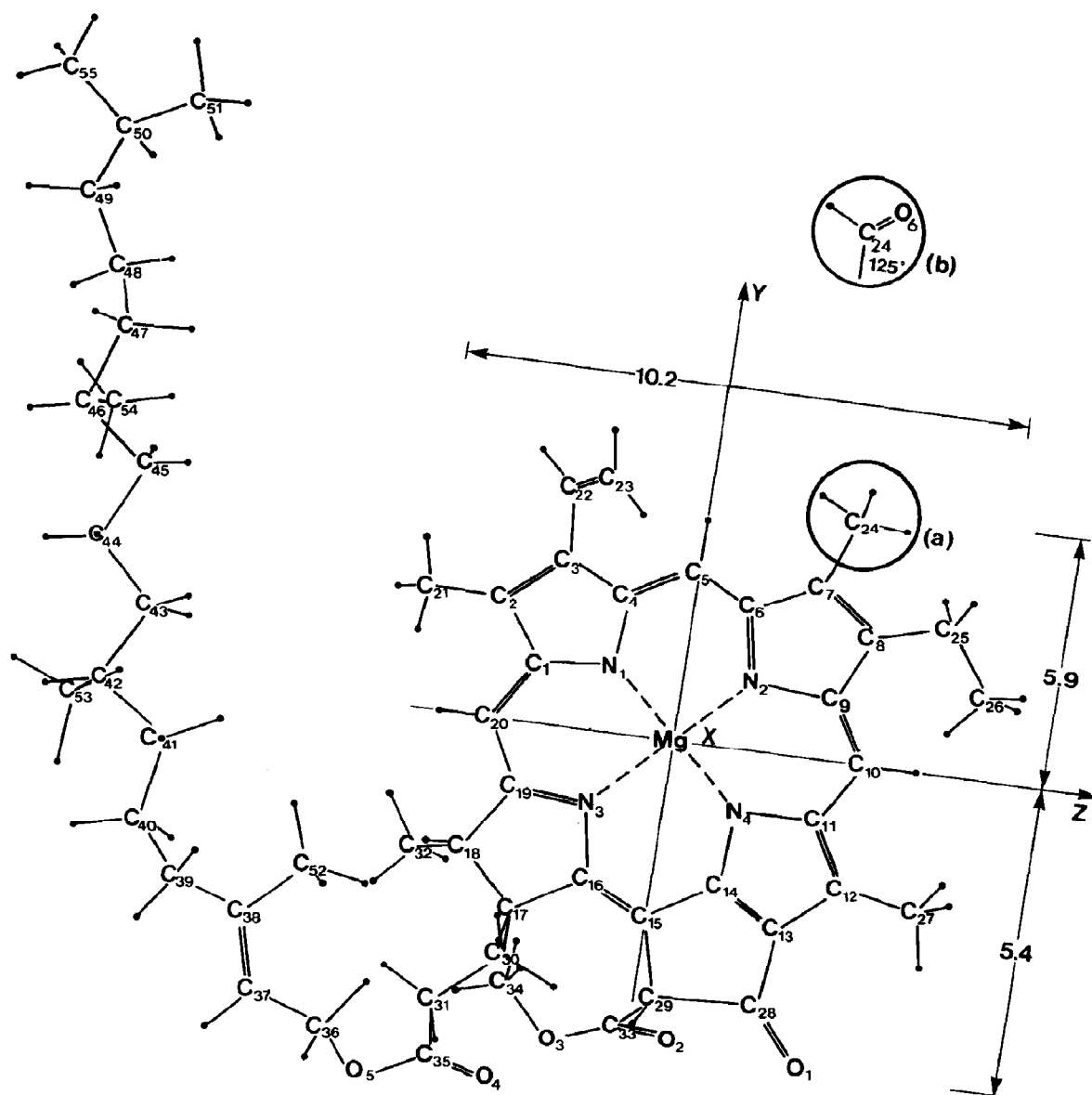


Fig. 1. Structure of chlorophyll based on the X-ray work of Kratky and Dunitz [16]. (a) Chl *a*, (b) Chl *b*. Distances in Å.

Table 1

Wave number positions ( $\text{cm}^{-1}$ ) of the C-H stretch vibrations of Chl *a*

System 1, part IV, fig. 3 [13]; system 2, part IV, fig. 8 [13]; system 3, part V, fig. 1 [15]; system 4, this work, fig. 3B; system 5, this work, fig. 2, mean spectrum, fig. 3A.

System	Spectrum	Aromatic CH		CH <sub>3</sub> degenerate stretch			CH <sub>2</sub> asymmetric stretch		
		3050– 3020	3019 2990	2989– 2965	2964– 2957	2956– 2949	2948– 2935	2934– 2925	2924– 2915
Description									
1. Multilayer									
	(B) 15 min after deposition				2957			2925	
	(E) 360 min after deposition				2957			2925	
2. Multilayer									
	(B) 6 h after deposition					2954			2922
	(D) 5 h under vacuum (0.1 Pa)					2954			2924
	(E) 16 h under vacuum (0.1 Pa)					2953			2923
3. Multilayer									
	(A) 25 min after deposition					2949		2925	
	(B) Vacuum (0.1 Pa), 75°C, 1 h					2954		2929	
	(C) H <sub>2</sub> O, 25°C, 2.5 h					2951		2929	
	(D) Dried, 25°C, 63 h				2959			2929	
	(E) Vacuum (0.1 Pa), 75°C, 6 h					2951			2924
4. Multilayer 2 h after deposition									
					2958				2921
5. Monolayer									
	(E') 47 min after deposition	3043	2998		2964	2954	2935		2923
	(I') Vacuum (0.1 Pa), 65°C, 2 h	3036		2978	2957	2948	2935 sh	2931	2922
	(P') H <sub>2</sub> O, 25°C, 10 h	3036	3005		2960	2952	2938	2929	2922
	(R') After 165 min	3031	3014	2982	2957	2953 sh	2938	2925	
	(V') Vacuum (0.1 Pa), 1.5 h, 25°C	3031		~ 2980	2958		2938	2925	
	(Z') Vacuum (0.1 Pa), 65°C, 1.5 h			2980	2960	2950	~ 2937 sh	2929	2921
	(ZZZ') After 3 h	3036	3008	~ 2980	2963	2956	~ 2935 sh	2929	2923
	Mean spectrum	3035	3004	2977	2957	~ 2953 sh	~ 2935 sh	2928	2923
Mean ± S.D.		3036 ± 4	3006 ± 7	2980 ± 2	2959 ± 3	2952 ± 2	2937 ± 2	2928 ± 2	2923 ± 1

properties of the aliphatic chain, the phytol chain is pointing out of the surface of the trough; in the figure it is pointing at the top. The organization of the monolayer is transferred intact on a hydrophilic MIR plate [15]. Thereafter, the monolayer organization is modified depending on the humidity content surrounding the sample.

The many different C-H groups of the chlorophyll molecule are illustrated in fig. 1. In this figure, we see six aliphatic CH<sub>3</sub> (C<sub>32</sub>, C<sub>51</sub>, C<sub>52</sub>, C<sub>53</sub>, C<sub>54</sub>, C<sub>55</sub>), three CH<sub>3</sub> on the porphyrin ring (C<sub>21</sub>, C<sub>24</sub>, C<sub>27</sub>), one CH<sub>3</sub> on the propyl group (C<sub>26</sub>), one CH<sub>3</sub> on the ester group (C<sub>34</sub>), 12 aliphatic CH<sub>2</sub> (C<sub>30</sub>, C<sub>31</sub>, C<sub>36</sub>, C<sub>39</sub>, C<sub>40</sub>, C<sub>41</sub>, C<sub>43</sub>,

C<sub>44</sub>, C<sub>45</sub>, C<sub>47</sub>, C<sub>48</sub>, C<sub>49</sub>), one CH<sub>2</sub> propyl on the porphyrin ring (C<sub>25</sub>), five aliphatic CH (C<sub>17</sub>, C<sub>18</sub>, C<sub>42</sub>, C<sub>46</sub>, C<sub>50</sub>), one aliphatic CH on the ring V (C<sub>29</sub>), two vinyl CH (C<sub>22</sub>, C<sub>37</sub>), one vinyl CH<sub>2</sub> (C<sub>23</sub>), and finally, three aromatic CH (C<sub>5</sub>, C<sub>10</sub>, C<sub>20</sub>). For Chl *b*, the CH<sub>3</sub> on C<sub>24</sub> is replaced by a formyl group.

All the different C-H groups will have different absorption patterns, and while it is difficult to make a detailed assignment of each C-H group, which would necessitate lengthy isotopic substitution, it is possible to assign most of the groups by comparing the spectra with model molecules. In table 2, we give the positions of some molecules

CH <sub>3</sub> symmetric stretch, aromatic	CH stretch	CH <sub>3</sub> symmetric stretch		CH <sub>2</sub> symmetric stretch	
				2865–	2857–
2914–	2899–	2879–	2871–	2858	2850
2900	2880	2872	2866		
			2866		2854
			2866		2854
			2869		2850
			2871		2852
			2869		2855
					2856
				2861	
				2861	
				2861	
					2856
~ 2905 sh			2871		2850
2908	2892	2877	2870		2849
~ 2911 sh	2893	2876	2866		2854
2907	2890		2869		2855
2905	2890		2866	2858	
2905	2890		2868		2853
2910	2890		2868		2852
2907	2889			2864	2851
2908	2890	2878	2868	2864	2852
2907 ± 2	2891 ± 2	2877 ± 1	2868 ± 2	2861 ± 2	2853 ± 2

whose absorption should match that of some of the functional groups of Chl molecules. To the right of this table, we list these groups. Some small displacements are expected because the model molecules do not match the Chl situation entirely. These molecules were chosen because the assignments of their bands are well documented [26–29]. In this table we notice that the positions of the bands of gaseous *n*-butane are different from those of CS<sub>2</sub> solution [22]; this is an indication that the dielectric environment of the absorbing groups will play a role in the positions of the bands.

To evaluate this phenomenon, Buckingham's equation [20], that uses the dielectric constant ( $\epsilon$ )

and refractive index ( $\eta$ ) to evaluate the solvent effects in infrared spectroscopy, is widely used. It was used by Bekarek et al. [21] to evaluate the frequency shifts of the carbonyl bands of Chl *a* in different solvents. In the monolayer organization, the appearance of many carbonyl components and the modification of these components with different aggregation states were explained by the variation of the dielectric milieu surrounding the different carbonyl groups [15]. The solvent effect or, more generally, the dielectric milieu should also influence the C-H stretching band, and this matter was studied by Cameron et al. [22] with *n*-octane in different solvents. They observed displacements

Table 2

Wave number positions ( $\text{cm}^{-1}$ ) of C-H stretch vibrations of model molecules and chlorophyll molecules

s, strong; m, medium; w, weak; sh, shoulder; v, very; b, broad; ia, inactive; sha, sharp; st, stretch; d, degenerate; a, asymmetric.

Compound	Ref.	3100– 3050	3050– 3030	3029– 3000	2999– 2965	2964– 2957	2956– 2949	2948– 2940	2939– 2925	2924– 2915
Benzene	26	CH st 3063 s	CH st 3047 ia							
CH st aromatic	27	3070 w	3030 sha							
1,3-Butadiene	26	CH <sub>2</sub> a-st 3101 s	CH st 3055 s		CH <sub>2</sub> s-st 2984 s					
Methyl acetate	26		CH <sub>3</sub> d-st 3035 m	CH <sub>3</sub> d-st 3005 m	CH <sub>3</sub> s-st 2966 s					
Toluene	28				CH <sub>3</sub> d-st 2980 vs					
Hexamethylbenzene	28						CH <sub>3</sub> d-st 2950			
Hexaethylbenzene	28		CH <sub>2</sub> a-st 3030 sh				CH <sub>3</sub> d-st 2950 sb			
<i>n</i> -Butane ( <i>trans</i> )	26				CH <sub>3</sub> d-st 2968 s				CH <sub>2</sub> a-st 2930 s	
<i>n</i> -Butane ( <i>gauche</i> )	26				CH <sub>3</sub> d-st 2968					CH <sub>2</sub> a-st 2920
<i>n</i> -Octane (gas)	22				CH <sub>3</sub> d-st 2969 s				CH <sub>2</sub> a-st 2933 vs	
<i>n</i> -Octane (CS <sub>2</sub> )	22						CH <sub>3</sub> d-st 2953 s			CH <sub>2</sub> a-st 2921 vs
Polymethylene	26									CH <sub>2</sub> a-st 2919 s
CH st. aliphatic	28									
Formaldehyde	26									
Acetaldehyde	26									
Chl <i>a</i> multilayer (1)	table 1					CH <sub>3</sub> d-st 2957			CH <sub>2</sub> a-st 2925	
Chl <i>a</i> multilayer (2)	table 1						2954		2923	
Chl <i>a</i> monolayer (mean spectrum)	table 1		3035	3004	2979	2957	2953		2935	2928
Chl <i>b</i> multilayer	table 3						2954		2926	
Chl <i>b</i> monolayer (mean spectrum)	table 3			3026 3017	2983 2970	2963 2958	2952		2939 2928	2922

of up to 15.3 and 11.3  $\text{cm}^{-1}$  from the vapor phase positions for the CH<sub>3</sub> degenerate stretching and CH<sub>2</sub> asymmetric stretch bands, respectively. To explain these displacements, the authors have used a variation of Buckingham's equation given by David and Hallam [23].

In the solid state, the dielectric milieu also influence the number of components and the position of the absorbing species. In solid methane, for

instance, the C-H stretch frequency gives one band situated at approx. 3010  $\text{cm}^{-1}$  for phase one, and for phase two, more than six components situated between 3026 and 3000  $\text{cm}^{-1}$  [24]. Orientation order also influences the position and number of absorbing species [25].

The conformation of the chain will also affect the position of the CH<sub>2</sub> groups. We can see from table 2 that for *trans-n*-butane, these groups are

2914– 2900	2899– 2890	2889– 2878	2877– 2866	2865– 2850	2849– 2830	2829– 2800	2799– 2750	Corresponding CH groups in Chl
								3 aromatic C-H: $C_5, C_{10}, C_{20}$ 2 vinyl C-H: $C_{22}, C_{37}$ 1 vinyl $CH_2$ : $C_{23}$ 1 $CH_3$ : $C_{34}$
CH <sub>3</sub> s-st 2900 s				2νδ 2850 sh 2νδ 2850 sh				3 aromatic CH <sub>3</sub> : $C_{21}, C_{24}, C_{27}$ 1 aromatic CH <sub>2</sub> -CH <sub>3</sub> : $C_{25}, C_{26}$
			CH <sub>3</sub> s-st 2870 s CH <sub>3</sub> s-st 2870 CH <sub>2</sub> s-st 2867 m CH <sub>3</sub> s-st 2867 w	CH <sub>2</sub> s-st 2853 ia CH <sub>2</sub> s-st 2860 CH <sub>2</sub> s-st 2852 m CH <sub>2</sub> s-st 2851 s				6 aliphatic CH <sub>3</sub> : $C_{32}, C_{51}, C_{52}$ $C_{53}, C_{54}, C_{55}$ 12 aliphatic CH <sub>2</sub> : $C_{30}, C_{31}, C_{36}, C_{39}$ $C_{40}, C_{41}, C_{43}, C_{44}$ $C_{45}, C_{47}, C_{48}, C_{49}$
		CH <sub>3</sub> s-st 2882 w CH <sub>2</sub> a-st 2883 ia				CH <sub>2</sub> s-st 2848 ia		6 aliphatic CH: $C_{17}, C_{18},$ $C_{29}, C_{42}, C_{46}, C_{50}$
	2900– 2880			CH <sub>2</sub> a-st 2843 vs			CH <sub>2</sub> s-st 2783 s	1 formyl CH
					CH st 2822 m			
			CH <sub>3</sub> s-st 2866 2870 2868	CH <sub>2</sub> s-st 2854 2852 2864 2852 2860				
2908	2890	2878						
			2873 2870	2863	2850		2762 2750	

situated  $10\text{ cm}^{-1}$  higher than in the *gauche* form. The CH<sub>3</sub> groups are unaffected by this mechanism, but being terminal groups, they will be more affected by the surroundings.

For the C-H vibrational stretch frequencies of Chl monolayers, we can expect displacements of the order of  $10\text{ cm}^{-1}$  for the aliphatic groups; similar displacements should also occur for the aromatic groups.

### 3.2. C-H vibrational bands of Chl *a* monolayer

The spectra of a monolayer of Chl *a* are given in fig. 2. Spectrum E' (\*) was taken 47 min after deposition. After heating the sample at  $65^\circ\text{C}$  under a vacuum of 0.1 Pa for 2 h, spectrum I' was taken. After putting the sample in water vapor at  $25^\circ\text{C}$  for 10 h, spectrum P' was taken; 115 min later spectrum R' was taken. After putting the

sample under a vacuum of 0.1 Pa at 25°C for 1.5 h, spectrum V' was taken. After drying the sample further by heating it at 65°C under a vacuum of 0.1 Pa for 1.5 h, spectrum Z' was taken, then, 230 min later, spectrum ZZZ' was taken. The position of the most reliable bands is given in table 1.

To delineate the zones of interest, we have compared in fig. 3 the spectrum of a monolayer of Chl *a* with that of a multilayer. The monolayer of Chl *a*, presented in fig. 3A, is the mean of the spectra given in fig. 2. In fig. 3B we give a typical spectrum of a multilayer of Chl *a* obtained 2 h after deposition. Since the intensity of the bands of a multilayer obtained by the MIR technique is not directly proportional to the number of layers [30] it is necessary to use a normalization procedure in order to compare both systems. We choose the CH<sub>2</sub> a-stretch band to do so because this band is the most intense and the most reliable of the C-H stretch bands. In fig. 3C, we give the difference between the two spectra. The zero position for the difference spectrum is situated at the 89 position on the % *T* scale.

If we compare the spectrum of the monolayer and that of the multilayer given in fig. 3A and B, respectively, we notice that the principal components absorb at about the same positions with the exception that there are more satellite features in the monolayer. We have observed the same phenomenon in the carbonyl region [15]. These satellite features will be displaced when the aggregation state is modified (fig. 2). The mobility of the satellite features is restricted to limited regions and these are given in table 1 along with the principal regions.

On the basis of table 2, and considering the displacement of the bands, we have divided the C-H stretch bands into seven main regions. These

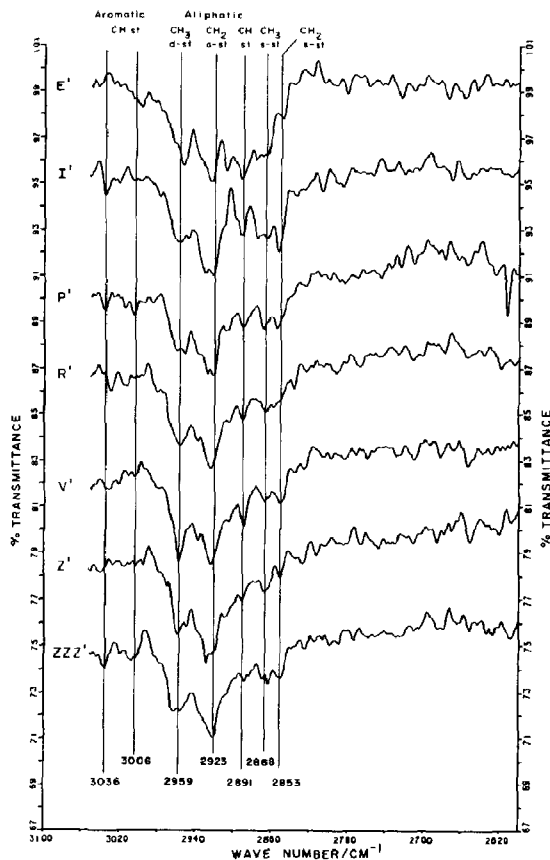


Fig. 2. Infrared spectra of the C-H region of Chl *a* monolayer ( $2 \times 1$  layer). The background of spectrum E' is close to 100% *T*. Each of the other spectra is displaced 4% *T*. (E') Sample, 47 min after deposition; (I') 30 min after heating at 65°C under vacuum (0.1 Pa) for 2 h; (P') 50 min after 10 h in water vapor bath at 25°C; (R') 165 min after; (V') 50 min after a vacuum (0.1 Pa) for 1.5 h at 25°C; (Z') 50 min after heating at 65°C under vacuum (0.1 Pa) for 1.5 h; (ZZZ') 280 min after.

regions are further divided in order to bring together the bands of the same vibrational origin in the same apparent dielectric milieu.

### 3.2.1. The 3050–2990 $\text{cm}^{-1}$ region

In this region the C-H vibrations are found on double-bonded carbons (table 2). For Chl *a* monolayers, we observe in this region two small bands situated at approx. 3036 and approx. 3067  $\text{cm}^{-1}$ . The intensities and positions of these bands

\* The numbering of the spectra follows that of part V of this series [15] because the spectra shown in this figure were taken along with those of part V. We have used primes (') to distinguish these spectra from those of the previous paper because they are not the same. The spectrometer setting is different and the time at which the spectra were taken is slightly different in both cases. For a better comparison between the time at which the spectra were taken, one may refer to the figure legends.



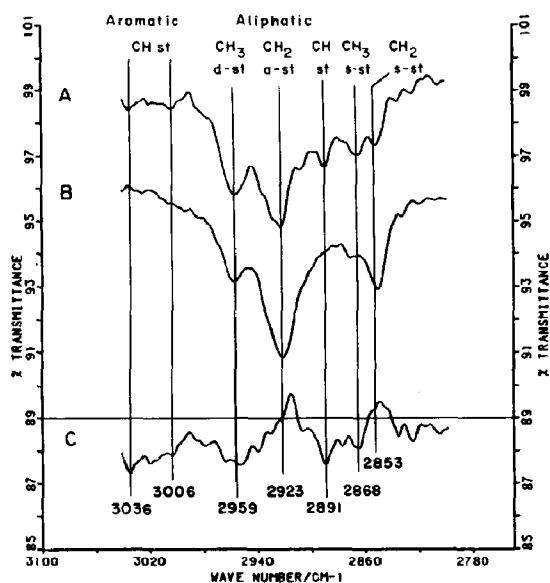


Fig. 3. Infrared spectra of the C-H region of Chl *a*. (A) Monolayer of Chl *a*. Mean spectrum obtained by averaging the spectra given in fig. 2 (see text). (B) Multilayer of Chl *a* ( $2 \times 40$  layers) obtained 2 h after deposition. The intensity of the 2921  $\text{cm}^{-1}$  band has been normalized to the intensity of the 2923  $\text{cm}^{-1}$  band of the monolayer. Scale displaced 4% *T*. (C) Difference between spectrum A and spectrum B. 0% *T* is situated at 89% *T*.

vary from spectrum to spectrum. The first band is most evident in fig. 2I' whereas the second one is in fig. 2P'. In the mean spectrum (fig. 3A), these bands, although weak because of the averaging procedure, are positioned at 3035 and 3004  $\text{cm}^{-1}$ . The position of the first band is in the region where other CH aromatic compounds absorb (table 2) and we assign the  $3036 \pm 4 \text{ cm}^{-1}$  band to the aromatic C-H on the porphyrin ring ( $C_5$ ,  $C_{10}$ ,  $C_{20}$ ). The second band, being situated at  $3006 \pm 7 \text{ cm}^{-1}$ , is more mobile than the first one and is assigned to the vinyl CH situated on  $C_{22}$  and  $C_{37}$  and to the degenerate (d)-stretch of the  $\text{CH}_3$  on  $C_{34}$ . These groups are quite different from one another; one vinyl group is attached to the porphyrin ring, the other vinyl group is in the middle of the phytol chain, the third group is a methyl on an ester of a small side chain. It is therefore understandable that any perturbations of the system will affect these groups differently and

the absorption of these groups will be delocalized; only when the dielectric milieu places the absorption in a close frequency range is the band seen.

In the multilayer system (fig. 3B) the bands in the 3050–2990  $\text{cm}^{-1}$  region are not apparent; this is due in part to the integrating mechanism that was mentioned earlier. It also seems that other factors are working on these bands, because, as we will see on other bands, the dielectric milieu affects the position of a band but not so much its intensity. One of these factors could be a symmetry factor. In the region from 3050 to 2990  $\text{cm}^{-1}$ , we notice that in the difference spectrum (fig. 3C), the absorption in the monolayer is stronger than in the multilayer. The C-H groups on  $C_5$ ,  $C_{10}$  and  $C_{20}$  are in a pseudo  $D_{4h}$  symmetry when the porphyrin ring is plane, and when in this symmetry, these C-H groups will not absorb strongly. When the planarity of the ring is decreased by a perturbation of the molecule, the symmetry will decrease and the absorption will increase. The organization of the molecules is more stable in the multilayers than in the monolayer and the planarity of the porphyrin ring will be less affected in the former, whereas in the latter, the porphyrin ring is subject to much stress which will deform it. This factor will make the aromatic C-H in the monolayer more active than in the multilayer.

Another factor that could influence the intensity in this region is the presence or absence of harmonic and combination bands originating from the 1650  $\text{cm}^{-1}$  region. We saw in part V [15] that the position and intensity of the bands in this region were modified when the aggregation state of the monolayer was modified.

### 3.2.2. The 2989–2949 $\text{cm}^{-1}$ region

In this region the main absorption is due to absorption of the degenerate stretch of aliphatic methyls (table 2). In both the multilayered and monolayered systems, we see in fig. 3 a neat band situated at approx. 2957  $\text{cm}^{-1}$ . This band is assigned to the degenerate stretch of the seven  $\text{CH}_3$  aliphatic groups situated on  $C_{26}$ ,  $C_{32}$ , and  $C_{51}$ – $C_{55}$ . The symmetric (s)-stretch of  $\text{CH}_3$  on  $C_{34}$  can also absorb in this region.

For the monolayer of Chl *a* (fig. 2), we see that the band in this region is split into many compo-

nents which are modified from one spectrum to another. The two principal components are situated at  $2959 \pm 3$  and  $2952 \pm 2$   $\text{cm}^{-1}$  (table 1). The separation between the two components is characteristic of the splitting occurring in phase transitions of aliphatic hydrocarbon compounds [29]. On the high-frequency side of the  $2959$   $\text{cm}^{-1}$  component, we observe on most of the spectra in fig. 2 a small feature situated at approx.  $2980$   $\text{cm}^{-1}$ . This position is too high for the  $\text{CH}_3$  aliphatic groups to absorb. Since this band is situated in the same frequency range as the  $\text{CH}_3$  d-stretch of toluene, the  $\text{CH}_3$  s-stretch of methyl acetate, and the  $\text{CH}_2$  s-stretch of butadiene, we assign the approx.  $2980$   $\text{cm}^{-1}$  band to the three d-stretch of the aromatic  $\text{CH}_3$  ( $\text{C}_{21}$ ,  $\text{C}_{24}$  and  $\text{C}_{27}$ ), to the s-stretch of the  $\text{CH}_3$  on  $\text{C}_{34}$ , and to the s-stretch of the  $\text{CH}_2$  of the vinyl group on  $\text{C}_{23}$ .

On the multilayer system (fig. 3B), one component is seen at  $2958$   $\text{cm}^{-1}$ . From the spectrum of the difference between the monolayer and the multilayer (fig. 3C), we notice, at  $2959$   $\text{cm}^{-1}$ , that the intensity of the absorption in the monolayer system is greater than that in the multilayer system. In the latter, the  $\text{CH}_3$  terminal groups are more mixed with the other groups in the system than those of the former, which pushes the absorption to lower frequency.

If we look at the pressure-area isotherms ( $\pi$ - $A$  curve) in fig. 4, we see that at a deposition pressure of  $20$   $\text{mN m}^{-1}$  the areas covered by one molecule of phytol and one molecule of Chl *a* are approx.  $31$  and approx.  $92$   $\text{\AA}^2$ , respectively. In a monolayer situation the phytol chain has ample space to move between the Chl molecules, whereas in a multilayer, the phytol chains are mixed together and this situation will hinder the movement of the chain and the molecule as a whole.

### 3.2.3. The $2948$ – $2915$ $\text{cm}^{-1}$ region

The asymmetric stretch of the aliphatic methylene groups absorbs in this region (table 2). For Chl *a*, the strongest band in the CH stretch region absorbs in this region at approx.  $2922$   $\text{cm}^{-1}$  (fig. 3). This band is assigned to the asymmetric stretch of the 12 aliphatic  $\text{CH}_2$  groups ( $\text{C}_{30}$ ,  $\text{C}_{31}$ ,  $\text{C}_{36}$ ,  $\text{C}_{39}$ – $\text{C}_{41}$ ,  $\text{C}_{43}$ – $\text{C}_{45}$ ,  $\text{C}_{47}$ – $\text{C}_{49}$ ). On the multilayer system, we observe (fig. 3B) only one large feature-

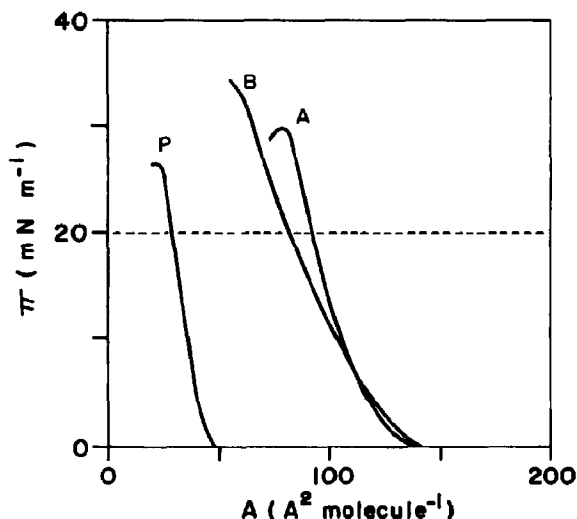


Fig. 4. Surface pressure-area isotherms of pure Chl *a* (A), pure Chl *b* (B), and phytol (P) taken at  $20^\circ\text{C}$ . Buffer, phosphate ( $10^{-3}$  M, pH 8.0). Spreading solvent, benzene. Deposition is done at a surface pressure,  $\pi$ , of  $20$   $\text{mN m}^{-1}$ .

less component situated at  $2921$   $\text{cm}^{-1}$ . On the monolayer system we observe in most cases (fig. 2) three components situated at approx.  $2936$ ,  $2927$  and  $2923$   $\text{cm}^{-1}$  (table 1). The last two components are the most intense ones, and in many cases are well resolved as in fig. 21'. The integrated absorption of this band is fairly constant throughout, but the intensity of the satellites does vary from one spectrum to the other. These satellite features can still be seen in the mean spectrum as shoulders on the main component situated at  $2923$   $\text{cm}^{-1}$  (fig. 3A). The presence of three components for this band, the separation between these components, and the modifications that occur from spectrum to spectrum could be the manifestation of crystalline field splitting, *gauche-trans* transition, change of the dielectric milieu surrounding the  $\text{CH}_2$  groups or any combination of the three. In any case, the variation of the band from spectrum to spectrum is an indication of the mobility of the phytol chain during the perturbation of the system.

When we compare the relative intensity in absorbance of the  $\text{CH}_3$  d-stretch band with the  $\text{CH}_2$  asymmetric stretch band in the mono- and multilayer systems we obtain the following: in the

monolayer system the intensity of the  $2957\text{ cm}^{-1}$  is 78% of that of the  $2923\text{ cm}^{-1}$  band; in the multilayer system, the intensity of the  $2958\text{ cm}^{-1}$  band is 54% of that of the  $2921\text{ cm}^{-1}$  band. These values can be compared with the number of CH groups in the  $\text{CH}_3$  and  $\text{CH}_2$  aliphatic groups of Chl *a* which is  $6 \times 3 = 18$  and  $12 \times 2 = 24$ , respectively; therefore, there are 75% as many CH species in the  $\text{CH}_3$  groups as there are CH species in the  $\text{CH}_2$  groups. From these values it is evident that the  $\text{CH}_3$  and  $\text{CH}_2$  groups are more separated in the monolayer than in the multilayer, and in the latter, there is a mixing of the phytol chain which will affect the  $\text{CH}_3$  groups and bring some absorption of these groups below  $2940\text{ cm}^{-1}$ .

#### 3.2.4. The $2914\text{--}2900\text{ cm}^{-1}$ region

The symmetric stretch of the aromatic methyls is situated in this region (table 2). In the monolayer spectra of Chl *a* a single band situated at approx.  $2908\text{ cm}^{-1}$  is observed. This band can be assigned to the s-stretch of the aromatic  $\text{CH}_3$  on  $\text{C}_{21}$ ,  $\text{C}_{24}$ , and  $\text{C}_{27}$ . In most cases the intensity of this band is low and this follows the intensity of the  $2980\text{ cm}^{-1}$  band, which was assigned to the degenerate stretch of the same aromatic  $\text{CH}_3$ . The separation between these two bands is also comparable to what has been observed for toluene (table 2). There is one exception in fig. 2E'; the intensity of the  $2908\text{ cm}^{-1}$  band is much stronger than in the following spectra; the reason for this higher intensity is probably some modifications occurring in the aggregation state at that moment, which influence the intensity of this band.

In the mean spectrum of the monolayer system, this band is situated at  $2908\text{ cm}^{-1}$  (fig. 3A). In the multilayer system (fig. 3B), some nonresolved absorption occurs.

#### 3.2.5. The $2899\text{--}2880\text{ cm}^{-1}$ region

The aliphatic methine groups absorb in this region (table 2). For the monolayer of Chl *a* we observe one band at  $2891\text{ cm}^{-1}$ . This position is constant with the different aggregation states, but its intensity, while weak, varies from one spectrum to the other. One exception to this rule is observed in spectrum E', where the intensity of this band is unusually high. The reason for this is probably the

same as for the preceding band at  $2908\text{ cm}^{-1}$ : there is some perturbation in the aggregation state that enhances momentarily the intensity of these two bands. The  $2891\text{ cm}^{-1}$  band is assigned to the six aliphatic C-H stretch components situated on  $\text{C}_{17}$ ,  $\text{C}_{18}$ ,  $\text{C}_{29}$ ,  $\text{C}_{42}$ ,  $\text{C}_{46}$  and  $\text{C}_{50}$ .

In the mean spectrum of the monolayer (fig. 3A), this band is situated at  $2890\text{ cm}^{-1}$ . In the multilayer system (fig. 3B), this band is not seen, and only low-intensity featureless absorption occurs. From the difference spectrum (fig. 3C) we notice that the intensity at  $2891\text{ cm}^{-1}$  is much stronger in the monolayer as compared to the multilayer. Due to the solvent effect, the frequency of a band is normally lowered. In this case, the intensity of the absorption occurring at a frequency lower than the  $2891\text{ cm}^{-1}$  band is not greater in the multilayer than in the monolayer; we can see in the difference spectrum (fig. 3C) that there is an increase in the intensity of the multilayer at approx.  $2915\text{ cm}^{-1}$ . Therefore, in the multilayer, the frequency of the CH aliphatic band is raised. This behavior, which is contrary to the normal behavior of solvent shifts, is not presently understood but is due to the mixing of the phytol groups.

#### 3.2.6. The $2879\text{--}2850\text{ cm}^{-1}$ region

The symmetric stretch of the aliphatic  $\text{CH}_3$  and  $\text{CH}_2$  of hydrocarbons is situated in this region (table 2). For the monolayer of Chl *a* several bands are found in this region, whose intensities vary from one spectrum to another (fig. 2). The intensity of the bands is low; the region covered is less than that for the asymmetric stretch bands, and the variation of the bands with the aggregation state is great (fig. 2). For these reasons, there is considerable overlap of the bands in this region and the separation between  $\text{CH}_3$  and  $\text{CH}_2$  bands that we have made is arbitrary. This separation is made at  $2865\text{ cm}^{-1}$  solely because this position separates the bands observed in the multilayer (fig. 3). Each of these regions is further divided into two, because, in many instances, we see doublets (fig. 2), the positions of which are fairly constant (table 1). In the mean spectrum, the positions of the  $\text{CH}_3$  s-stretch components are situated at  $2878$  and  $2868\text{ cm}^{-1}$ , and at  $2864$  and  $2852\text{ cm}^{-1}$  for the  $\text{CH}_2$  s-stretch ones.

In the multilayer system, two bands are observed: one at 2871 and the other at 2850  $\text{cm}^{-1}$  (fig. 3C), the first for the  $\text{CH}_3$  s-stretch and the second for the  $\text{CH}_2$  s-stretch. Depending on the experimental conditions these two bands are sometimes not resolved as in fig. 4 of ref. 11 and fig. 1 of ref. 15, and they are sometimes partially resolved as in fig. 3 of ref. 13. Because of the nature of the vibration, the symmetric stretch vibrations are more sensitive to the perturbation of the chain, and since the buildup of a multilayer is different for different experiments, the intensity pattern will be different for each sample.

### 3.2.7. The region below 2850 $\text{cm}^{-1}$

In this region we observe, especially below 2750  $\text{cm}^{-1}$ , some small bands whose intensities change from spectrum to spectrum. These small bands can originate from the harmonic or combination of bands situated in the 1400  $\text{cm}^{-1}$  region where deformation bands of the C-H groups occur. The intensity of these bands should fluctuate more than the stretching bands but no study has been made in this region. There is also the perturbation that the monolayer suffers when some water molecules depart or are introduced into the system. These local perturbations will modify the refractive index of the system and modify the incident beam as it passes through the sample. The sharp peak situated at 2613  $\text{cm}^{-1}$  on spectrum P' (fig. 2) is the strongest manifestation of this kind of perturbation that is occurring at that moment. This perturbation, which is analogous to what can be observed in a phase transition of a crystalline organic solid [24,25], is caused by the departure of the water molecules trapped in the monolayer after the water vapor bath. Above 2850  $\text{cm}^{-1}$  this kind of perturbation is also apparent but not enough to mask the absorption of the genuine vibrations which are confined to well defined regions (table 1).

### 3.3. C-H vibrational bands of Chl *b* monolayer

The spectra of a monolayer of Chl *b* are given in fig. 5. The spectrum E' (see footnote, p. 234) was taken 45 min after deposition. After heating the sample for 1.5 h at 65°C under a vacuum of

0.1 Pa, spectrum I' was taken. After the sample was under the influence of water vapor for 24 h at 25°C, spectrum M' was taken. After drying the sample again at 65°C under a vacuum of 0.1 Pa for 1.5 h, spectrum Q' was taken. Spectrum Z is the mean of the preceding spectra. The position of the most reliable bands is given in table 3.

The CH groups of Chl *b* will absorb in the same frequency range as those of Chl *a*, except for the CH of the formyl group which appears at lower frequency (fig. 5). The main difference between the monolayers of Chl *a* and that of Chl *b* lies in the aggregation of the two molecules. As we saw in part V [15], the formyl group will play a role in the aggregation of the monomolecular organization of Chl *b*. In a fresh multilayer or a fresh monolayer, the water molecules present be-

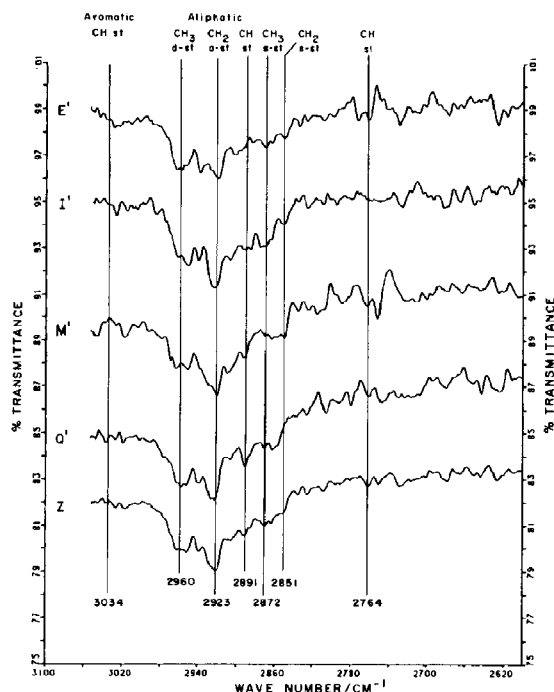


Fig. 5. Infrared spectra of the C-H region of Chl *b* monolayer ( $2 \times 1$  layer). The background of spectrum E' is close to 100% *T*. Each of the other spectra is displaced 4% *T*. (E') Sample, 45 min after deposition; (I') 30 min after heating at 65°C under vacuum for 2.5 h; (M') 30 min after 24 h in water vapor bath at 25°C; (Q') 30 min after heating at 65°C under vacuum (0.1 Pa) for 1.5 h; (Z) mean of the above spectra.

tween the porphyrin planes are linked on one side to the magnesium atom via coordinate bonds and on the other side with the CO of the formyl group in the case of Chl *b*, and with the  $\pi$ -electron network in the case of Chl *a*.

### 3.3.1. The 3050–2990 $\text{cm}^{-1}$ region

The intensities of the bands of Chl *b* in this frequency range are weaker than those of Chl *a* because the porphyrin ring is less affected in the former than in the latter. The reasons for this behavior can be understood if we look at the models that we have proposed in part V for the monolayer of Chl *a* and Chl *b* [15]. For Chl *a*, some water molecules are linked to the  $\pi$ -electrons of the porphyrin ring by hydrogen bonds. For Chl *b*, the water molecules are linked to the oxygen of the formyl group. The departure of the water molecules or their reintroduction will have a greater effect on the porphyrin of Chl *a* than on that of Chl *b* because water is linked directly to the porphyrin of Chl *a* and only indirectly to that of Chl *b*.

### 3.3.2. The 2989–2949 $\text{cm}^{-1}$ region

The positions of the three components forming the band (fig. 5) are the same as those of Chl *a* except that on the spectra of Chl *b* we observe, most of the time, the three components, whereas in Chl *a*, we observe one main component and one satellite feature at a time.

The methyl groups are terminal groups and therefore are quite sensitive to any perturbations from the environment. The presence of stronger components for the monolayer of Chl *b* than for that of Chl *a* indicates that more orientations are favored for the monolayer of Chl *b* than for that of Chl *a*. This is an indication that the monolayer of Chl *b* is less stable than that of Chl *a*. The difference in stability is due to the nature of the hydrogen bond formations situated between the water and Chl molecules, these bonds are weaker in the former than in the latter. We have arrived at the same conclusion from the study of the carbonyl region [15].

### 3.3.3. The 2948–2915 $\text{cm}^{-1}$ region

The  $2939 \pm 1 \text{ cm}^{-1}$  band is stronger in Chl *b*

than in Chl *a*. In the mean spectrum of the latter we see only a small shoulder (fig. 3A) whereas for the former we see a well-defined satellite feature (fig. 5Z). The reason for this situation is not obvious, but could arise from the appearance of the harmonic and combination of bands appearing in the  $1500 \text{ cm}^{-1}$  region. In this region, the bands are stronger for the monolayer of Chl *b* than for that of Chl *a* [15]. The cause could also be the arrangement of the conformers of the phytol chain which could be different in both cases.

### 3.3.4. The 2829–2750 $\text{cm}^{-1}$ region

The absorption of the C-H of the formyl group is situated in this region (table 2). On the spectra of the monolayer of Chl *b* (fig. 5), we see in this region some well-defined bands at 2774, 2763 and  $2730 \text{ cm}^{-1}$  on spectrum E' and at 2764 and  $2753 \text{ cm}^{-1}$  on spectrum M'. On the other spectra, the absorption is less evident. We assign the approx.  $2764 \text{ cm}^{-1}$  band to the C-H of the formyl group. Why does this band vary so much from one spectrum to the other? The answer to this question lies in the nature of this group: on the hydrogen of this group resides a small positive charge where a weak hydrogen bond can be made, and depending on the orientation of the molecules, the strength of this bond will be more or less strong and therefore the CH band will be more or less displaced; the carbonyl group next to the hydrogen can also form some hydrogen bonds [15] and by doing so will weaken the CH bond next to it; this phenomenon will also displace the CH band.

On a multilayer of Chl *b* [11,15] or in solution [1], there is no evident absorption in this region. The reason for this behavior is that the absorption is less localized than that of the monolayer.

## 4. Conclusion

The C-H stretch region of the chlorophyll molecule was considered unattractive because of its numerous groups giving rise to only 3 to 4 bands without structure when the molecules are in solution or when they are in a multilayer; however, in a monolayer system, it gives more than seven bands, most of which are composed of several components.

Table 3

Wave number positions ( $\text{cm}^{-1}$ ) of C-H stretch vibrations of chlorophyll *b*

System 1, part V, fig. 8; system 2, this work, fig. 5.

System	Spectrum	Aromatic CH		CH <sub>3</sub> degenerate stretch			CH <sub>2</sub> asymmetric stretch		
		3050– 3020	3019 2990	2989 2965	2964– 2957	2956 2949	2948– 2935	2934– 2925	2924– 2915
Description									
1. Multilayer									
(B) 20 min after deposition						2952			2924
(F) Vacuum (0.1 Pa), 75°C, 2.5 h									
(G) H <sub>2</sub> O, 75°C, 9 h					2957			2929	
(K) Vacuum (0.1 Pa), 25°C, 15 h						2952			2925
2. Monolayer									
(E') 45 min after deposition	3029				2963 2958	2953	2939	~ 2928 sh	2920
(I') Vacuum (0.1 Pa), 65°C, 2.5 h	3026			2985	2962	2951	2940		2924
(M') H <sub>2</sub> O vapor, 25°C, 24 h	3046	3018		2979 2970	2964	2952	2938	~ 2929 sh	2921
(Q') Vacuum (0.1 Pa), 65°C, 1.5 h				2977	2958		2939	2928	2923
Mean spectrum	3026	3017		2983 2970	2963 2958	2952	2939	2928	2922
Mean ± S.D.	3034 ± 11	3018		2978 ± 6	2960 ± 3	2952 ± 1	2939 ± 1	2929 ± 1	2923 ± 2

In the monolayer system of Chl *a*, the bands are divided into two groups: the aliphatic stretch absorption composed of five bands is situated mostly below  $2965 \text{ cm}^{-1}$ , and the aromatic stretch absorption, composed of more than four low-intensity bands, is situated between 3050 and  $2900 \text{ cm}^{-1}$ . Some of the latter are mixed with some of the former.

When a monolayer of Chl *a* or Chl *b* is perturbed by hydration or dehydration processes, three types of movement are identified in the molecules: the movement of the phytol chain, the movement of the porphyrin ring, and the tilt of the porphyrin ring. The first one is seen on the aliphatic bands where the separation between the components is comparable to what has been observed in solid hydrocarbons at low temperature. In the case of hydrocarbons the separation between the components has been interpreted as crystalline field splitting. In the Chl monolayers, the situation is

similar and we interpret the organization that prevails in the monolayer as a crystalline-like organization of the phytol chain. This organization is quite fragile because the intensity of the components varies from one spectrum to another when the monolayer is perturbed. The second one is seen on the aromatic bands, especially on the approx.  $3036 \text{ cm}^{-1}$  band, where the displacement of the bands and the variation of their intensities are indications of the deformation of the planarity of the porphyrin ring. The third kind of movement is the tilt of the porphyrin plane. This movement is particularly evident on the CH band of the formyl group of Chl *b* where the variation of the intensity of this band is the manifestation of the mobility of this group which can come from the tilting of the porphyrin ring. This kind of movement is most evident on the carbonyl groups and has been fully discussed in the preceding paper [15].

In a multilayer of Chl *a*, the aromatic bands are

CH <sub>3</sub> symmetric stretch, aromatic	CH stretch	CH <sub>3</sub> symmetric stretch	CH <sub>2</sub> symmetric stretch		CH formyl
			2865–	2857–2829–	
2914–	2899–	2879–	2858	2850	2829–
2900	2880	2866			2750
		2870	2859		
		2874	2862		
		2874	2859		
2904		2870		2850	2774 2763
2908	~ 2890	~ 2871	2864	2852	
2911	2892		2864	2851	2817 2764 2753
2906	2891	2872	2863		
2905	2891	2870	2863	2850	2762 2750
2907 ± 3	2891 ± 1	2872 ± 2	2862 ± 2	2851 ± 1	

not clearly observed, and only some broad featureless absorption is seen. The aliphatic stretch bands of the CH<sub>3</sub> groups are less intense than in the monolayer situation. The spectrum of such a system is much more stable than the monolayer organization. These observations are an indication that the phytol chains are mixed in a multilayer organization that stabilizes the system so that the deformation of the porphyrin ring is inhibited. Furthermore, these phytol chains will act as a solvent for the different groups they encounter giving solution-like patterns for the absorption. In a monolayer organization, the Chl molecules are separated from one another; the movement of the molecules will be less inhibited so that the positions of the bands are more defined.

In a fresh monolayer of Chl *a* or Chl *b*, the oxygens of the molecules are fixed to the MIR plate via hydrogen bonds, some water molecules are present between the porphyrin planes and by a

hydrophobic process the phytol chain will be like a column perpendicular to the plate. As the water molecules recede from the system, the phytol chains will collapse and in so doing the CH aliphatic groups encounter other groups in the monolayer. This situation will modify the intensity of the different components of the C-H aliphatic and aromatic stretch bands.

When the phytol chain is displaced, the planarity of the porphyrin ring is under stress that will deform it. Another stress that the porphyrin ring encounters is the departure of the water molecules. All these perturbations will affect the porphyrin ring and so the intensity of the aromatic stretch bands will be modified.

To obtain unambiguous assignments of all the C-H groups in the Chl molecules would necessitate isotopic substitutions at specific sites in the molecule. This task is lengthy. We have used an alternative approach. In this infrared study of the CH

stretch vibrations of the monolayer of Chl *a* and Chl *b* we have identified several bands which were not seen under experimental conditions which were different. The absorption of all the C-H groups can be classified into these bands. We have also identified some movements of the molecules in the monolayers which are inhibited when the molecules are in a multilayer or when they are in solution although it is difficult at this stage to be specific as to the movement of all the 72 different C-H groups in the Chl molecules.

## Acknowledgements

This work was supported by the National Sciences and Engineering Research Council of Canada and by the Fonds F.C.A.C. du Québec.

## References

- 1 J.J. Katz, R.C. Dougherty and L.G. Boucher, in: *The chlorophylls*, eds. L.P. Vernon and G.R. Seely (Academic Press, New York, 1966) ch. 7.
- 2 K. Ballschmiter and J.J. Katz, *Nature* 220 (1968) 1231.
- 3 J.J. Katz, and K. Ballschmiter, *Angew. Chem. Int. Edn.* 7 (1968) 286.
- 4 K. Ballschmiter, T.M. Cotton, H.H. Strain and J.J. Katz, *Biochim. Biophys. Acta* 180 (1969) 347.
- 5 K. Ballschmiter and J.J. Katz, *J. Am. Chem. Soc.* 91 (1969) 2661.
- 6 J.P. Dodelet, J. LeBrecht, C. Chapados, and R.M. Leblanc, *Photochem. Photobiol.* 31 (1980) 143.
- 7 K. Ballschmiter and J.J. Katz, *Biochim. Biophys. Acta* 256 (1972) 307.
- 8 T.M. Cotton, P.A. Loach, J.J. Katz and K. Ballschmiter, *Photochem. Photobiol.* 27 (1978) 735.
- 9 G. Sherman and S.-F. Wang, *Nature* 212 (1966) 588.
- 10 G. Sherman and S.-F. Wang, *Photochem. Photobiol.* 6 (1967) 239.
- 11 R.M. Leblanc and C. Chapados, *Biophys. Chem.* 6 (1977) 77.
- 12 C. Chapados and R.M. Leblanc, *Chem. Phys. Lett.* 49 (1977) 180.
- 13 C. Chapados, D. Germain and R.M. Leblanc, *Biophys. Chem.* 12 (1980) 189.
- 14 C. Chapados, D. Germain and R.M. Leblanc, *Can. J. Chem.* 59 (1981) 2402.
- 15 C. Chapados and R.M. Leblanc, *Biophys. Chem.* 17 (1983) 211.
- 16 C. Kratky and J.D. Dunitz, *J. Mol. Biol.* 113 (1977) 431.
- 17 S.M. de B. Costa, J.R. Froines, J.M. Harris, R.M. Leblanc, B.H. Orger, and G. Porter, *Proc. Roy. Soc. Lond.* 326 (1972) 503.
- 18 R.M. Leblanc, G. Galinier, A. Tessier, and L. Lemieux, *Can. J. Chem.* 52 (1974) 3723.
- 19 H.H. Strain and W.A. Svec, in: *The chlorophylls*, eds. L.P. Vernon and G.R. Seely (Academic Press, New York, 1966) ch. 2.
- 20 A.D. Buckingham, *Proc. Roy. Soc. A* 248 (1958) 169; *Proc. Roy. Soc. A* 255 (1960) 32; *Faraday Soc. Trans.* 56 (1960) 753.
- 21 V. Bekarek, M. Kaplanova, J. Socha, *Stud. Biophys. Berlin, Band 77* (1979) 21.
- 22 D.G. Cameron, S.C. Hsi, J. Umemura and H.H. Mantsch, *Can. J. Chem.* 59 (1981) 1357.
- 23 J.G. David and H.E. Hallam, *Spectrochim. Acta* 23A (1967) 593.
- 24 C. Chapados and A. Cabana, *Can. J. Chem.* 50, 21 (1972) 3521.
- 25 C. Chapados and A. Cabana, *Chem. Phys. Lett.* 7, 2 (1970) 191.
- 26 T. Shimanouchi, in: *Tables of molecular vibrational frequencies. Consolidated vol. 1* (Nat. Stand. Ref. Data Ser., Nat. Bur. Stand., U.S.) 39 (1972) p. 164.
- 27 L.J. Bellamy, in: *The infrared spectra of complex molecules* (Chapman and Hall, London, 1975).
- 28 N.L. Alpert, W.E. Keiser and H.A. Szymanski, in: *IR, Theory and Practice of Infrared Spectroscopy* (Plenum/Rosetta edition, New York, 1973) ch. 5.
- 29 H.L. Casal, D.G. Cameron and H.H. Mantsch, *Can. J. Chem.* 61 (1983) 1736.
- 30 T. Takenaka, K. Nogami, H. Gotoh and R. Gotoh, *J. Colloid Interface Sci.* 35 (1971) 395.